FACTORS INFLUENCING TENSILE MECHANICAL PROPERTIES OF Al-7Si-Mg CASTING ALLOYS A356/7

Heinrich Möller[1], Gonasagren Govender[1], Waldo Stumpf[2]

[1]CSIR (Council for Scientific and Industrial Research); Pretoria, 0001, South Africa

[2]Department of Materials Science and Metallurgical Engineering, University of Pretoria; Pretoria, 0001, South Africa

Keywords: Al-7Si-Mg alloys, Heat treatment, Mechanical properties

Abstract

Factors that influence the tensile mechanical properties of Al-7Si-Mg alloys A356/7 are critically analyzed. Different casting methods (SSM-HPDC, gravity die casting and investment casting), chemical composition variations and different temper conditions are considered. It is shown that the casting method employed has an influence on the primary α-Al structure, but does not influence the age-hardening response. The most important elements that influence mechanical properties are magnesium and iron. An equation to convert Vickers hardness to 0.2% proof stress in different temper conditions using the strain hardening exponent is proposed. Linear correlations between hardness, strength and (at% Mg-content available for precipitation hardening)$^{1/2}$ are found. It is shown that ASTM Standard B969-10 needs to be revised.

Introduction

Conventional casting alloys Al-7Si-Mg A356/7 contain between 6.5 and 7.5% Si, together with 0.25-0.7% Mg and are used for critical castings in aircraft such as the engine support pylons, while automotive components include wheels and cylinder heads [1]. With the advent of semi-solid metal (SSM) processing, the Al-7Si-Mg alloys soon became the most popular alloys for study [2]. This is due to their good castability and fluidity imparted by the large volumes of the Al-Si eutectic, with the additional advantage of the castings being age-hardenable to improve strength [1]. The aim of SSM-processing is to obtain a semi-solid structure which is free of dendrites and with the solid constituent present in a near spherical form.

The chemical composition limits for alloys A356, A357 and F357 are shown in Table I [3]. International standards for aluminium alloys often permit significant fluctuations in the content of alloying elements. The main difference between alloy A356 and the F357 alloy lies in the magnesium content, whereas the main difference between alloys F357 and A357 is their beryllium content (Table 1). The addition of beryllium to this alloy system (e.g. alloy A357) leads to a change in the morphology of the iron-rich intermetallics, which results in slightly better ductility [4]. The Be-containing alloys are gradually being phased out in many applications due to the carcinogenic effects of beryllium, particularly at higher concentrations used during make-up of the alloys.

It has been proposed that the heat treatment regimes for conventionally liquid cast A356/7 alloys with dendrites are not necessarily the optimal ones for SSM-cast alloys, as the different microstructure and solidification history of SSM components should be considered [5]. The American Society for Testing and Materials (ASTM) Standard B969 from 2010 named "*Standard Specification for Aluminum-Alloy Castings Produced by the Squeeze Casting, Thixocast and Rheocast Semi-Solid Casting*

Processes" recommends heat treatment parameters for SSM-cast A356 and A357 as shown in Table II.

Table I. Chemical composition limits (in wt%) for alloys A356, A357 and F357 [3]

		Si	Mg	Fe	Cu	Mn	Ti	Be
A356	Min	6.5	0.25	-	-	-	-	-
	Max	7.5	0.45	0.20	0.20	0.10	0.20	-
A357	Min	6.5	0.40	-	-	-	0.10	0.04
	Max	7.5	0.70	0.20	0.20	0.10	0.20	0.07
F357	Min	6.5	0.40	-	-	-	0.04	-
	Max	7.5	0.70	0.10	0.20	0.10	0.20	0.002

Table II. ASTM B969-10 recommended T6 heat treatment parameters for semi-solid thixocast and rheocast castings

Alloy	Solution heat treatment		Precipitation heat treatment	
	Metal temp. ± 5°C	Time at temp. (h)	Metal temp. ± 5°C	Time at temp. (h)
A356	540	4-10	160	3-6
A357	540	10	170	6

Recommendations on natural pre-aging and its influence on subsequent artificial aging are not included in this standard.

The aim of this paper is to investigate the influence of factors such as casting method, chemical composition variations and heat treatment on the tensile mechanical properties of these alloys. An equation to convert Vickers hardness to 0.2% proof stress in different temper conditions using the strain hardening exponent is proposed. Finally, the applicability of ASTM Standard B969-10 is determined.

Experimental

The Council for Scientific and Industrial Research (CSIR) rheocasting process [6] was used to prepare SSM slurries of Sr-modified A356 and F357. Plates with varying Mg-contents [7-11] and automotive brake callipers [12] were cast using either a 50, 130 or 630 ton clamping force high pressure die casting (HPDC) machine. In order to study these alloys with dendritic microstructures, gravity die cast (GDC) automotive brake callipers [12] and investment cast (IC) plates [13] were used. The "traditional heat treatment of 540°C for 6 h and artificial aging for 170°C for 6 h, as well as CSIR developed [7-12] shortened heat treatments of 540°C for 1 h, natural pre-aging (NA) of 0-120 h and artificial aging for 180°C for 4 h were employed.

The tensile properties of the alloys were determined using an INSTRON 1342/H1314 with 25 kN load cell capacity and an INSTRON Model 2620-602 extensometer with gauge length of 12.5mm. To determine the 0.2% proof stress (YS), a stress rate of 10MPa/s was used and for the ultimate tensile stress (UTS) determination a displacement rate of 10mm/min. These parameters were selected based on ASTM standard E8M-04. The extensometer was removed during tensile testing after reaching the 0.2% plastic strain value (typically after 1-2% strain) to prevent damage to the extensometer in the case of premature fracture. The % elongation after fracture was calculated in accordance with ASTM standard E8M-04, where gauge marks were drawn with ink on the tensile specimens. After fracture, the ends of the fractured specimen were fitted together carefully and the distance between the gauge marks measured. Tensile specimens were machined from the plates and brake callipers and can be seen elsewhere [7-12].

Results and discussion

A lower increase in strength with bulk Mg-concentration has been observed for alloy F357 when compared to alloy A356 [10,14]. Taylor and co-workers [14] determined the matrix Mg-content of A356 and F357 alloys (the Mg-concentration in solid solution after solution treatment at 540°C) by using electron probe microanalysis (EPMA). In the low Mg-alloys (A356), it was found that the final matrix Mg concentration equaled the bulk Mg-content of the alloy. This implies that, during solution treatment, all the as-cast Mg_2Si for strengthening was dissolved, and that the Mg-containing π-$Al_8FeMg_3Si_6$ intermetallic was also dissolved. As the alloy's Mg-content increased, the matrix Mg-levels did not reach the bulk values. Since very little Mg_2Si is expected to remain after the solution treatment, this phenomenon is likely due to the increased stability of the π-phase as the alloy Mg-content is increased. Deviation from full dissolution of Mg in the matrix occurred at approximately 0.4% Mg for alloys containing ~ 0.10% Fe [10,14]. The data from Taylor and co-workers [14] can be used to estimate the Mg-concentration available for precipitation hardening for the bulk compositions [12]:

Make y = wt% Mg available for precipitation hardening
    x = Bulk wt% Mg-content of alloy

For $0.25 \leq$ Bulk Mg ≤ 0.4

$$y = x \qquad (1)$$

For $0.4 \leq$ Bulk Mg ≤ 0.7

$$y = -0.25x^2 + 0.665x + 0.1755 \qquad (2)$$

The effects of Mg on the yield strength can be understood in terms of the age-hardening process. It is known [15] that the increment of the yield strength (ΔYS) is determined by the volume fraction (f) of shearable and non-shearable precipitates

$$\Delta YS = Constant \times (f)^{1/2} \qquad (3)$$

Provided that all of the Mg is available for precipitation hardening (i.e. calculated by equations 1 and 2 and converting from wt% to at% Mg), then ΔYS should be proportional to (at% Mg available for precipitation hardening)$^{1/2}$ – eq. 3 [15]. Therefore, taking the YS data points from SSM-HPDC alloys [7-11] as well as data

points from the literature [16,17] and plotting them against (at% Mg available for precipitation hardening)$^{1/2}$, a linear relationship is obtained as shown in Fig. 1 for the traditional T6 heat treatment.
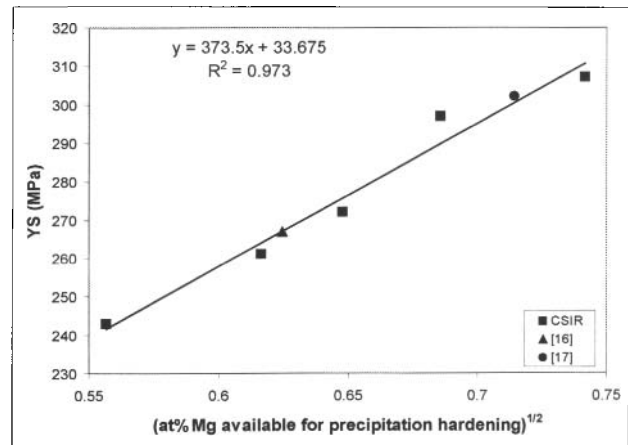

Figure 1. 0.2% YS as a function of (at% Mg-concentration available for precipitation hardening)$^{1/2}$ for the traditional T6 heat treatment.

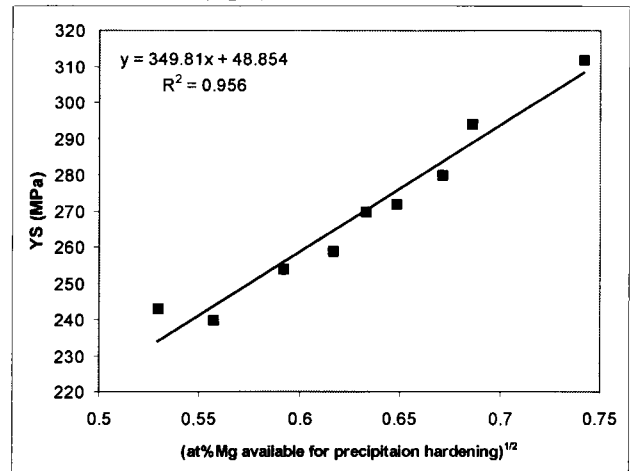A similar linear correlation is found when using the shortened CSIR heat treatments (Fig. 2).

Figure 2. 0.2% YS as a function of (at% Mg-concentration available for precipitation hardening)$^{1/2}$ for the short CSIR T6 heat treatment (540°C-1h,{20-120h}NA, 180°C-4h).

The shortened CSIR heat treatments were additionally applied on SSM-HPDC plates and brake callipers, IC plates and GDC brake callipers. In order to make comparisons between the different plates and brake callipers, Vickers hardness (VHN) was used instead of yield strength (as was done in Figs. 1 and 2) due to the lack of tensile data for IC plates (Fig. 3). Hardness generally correlates better with UTS than with YS since significant plastic deformation occurs with both hardness and UTS determination [18]. Figure 3 is therefore only used as a convenient method of making comparisons of the heat treatment response of Al-7Si-Mg castings produced by different casting techniques. It can be seen that a good linear correlation is achieved in Fig. 3.
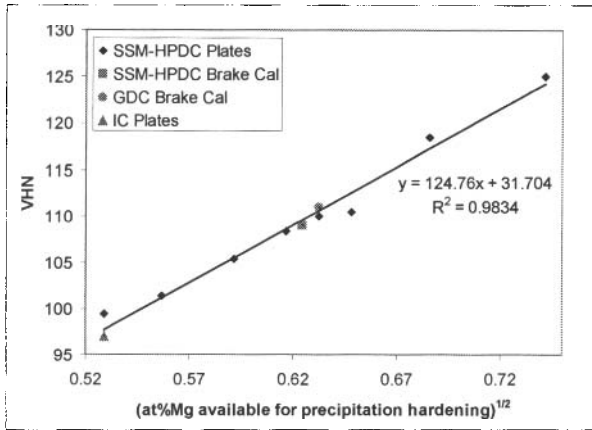
468

Figure 3. VHN as a function of (at% Mg-concentration available for precipitation hardening)$^{1/2}$ for the (540°C-1h,{20-120h}NA, 180°C-4h) T6 heat treatment applied to SSM-HPDC plates and brake callipers, as well as GDC brake callipers and IC plates.

The Si-contents of the alloys used in Figs. 2,3 varied between 6.6-7.3% [7-13] i.e. covering almost the whole range of 6.5-7.5% allowed in the specification (Table 1). Figures 2 and 3 therefore implies that the hardness of Al-7Si-Mg alloys in the T6 temper condition is controlled primarily by the Mg-content available for precipitation hardening after solution treatment and is independent of the casting technique used (i.e. dendritic or globular primary α-Al microstructure). The insignificant influence of Si-content variation is due to the fact that these Al-7Si-Mg casting alloys contain an excess Si that is required to form the strengthening β''-precipitates, which has a Mg:Si ratio of 1.1-1.2 [19]. The other important alloying element controlling the age-hardening capacity of (dendritic and globular) Al-7Si-Mg alloys is iron. The data points in Figs. 1-3 are all for alloys containing ~ 0.1% Fe. Higher Fe-contents (especially in alloys containing > 0.40% Mg) will result in a reduced response to age-hardening due to the stability of the π-Al$_8$FeMg$_3$Si$_6$ phase [10,14]. Therefore, provided that the maximum quantity of the alloy's Mg is placed into solid solution during solution treatment (which might take longer than 1 h at 540°C for dendritic alloys with a very coarse dendritic microstructures such as in large sand castings), and the alloy's Fe content is within specification (but preferably ~ 0.1%), the response to age hardening of Al-7Si-Mg alloys should be independent of the processing technique used.

As mentioned earlier, direct correlations between yield strength and hardness generally contain an appreciable amount of scatter. This is due to the fact that strain associated with a Vickers indentation is approximately 8% for a variety of strain hardening alloys and hardness therefore generally correlates better with UTS than with YS [18]. The YS and UTS as a function of the Vickers hardness for this work (F, T4, T5 and T6 temper conditions) [7-12] are plotted in Figures 4 and 5 respectively.
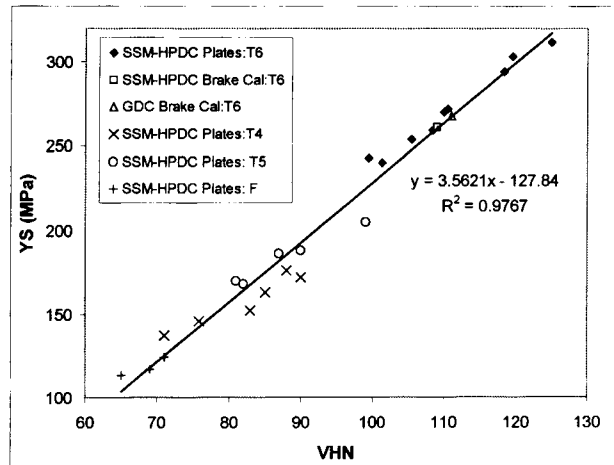

Figure 4. Correlation between YS and VHN for Al-7Si-Mg alloys in the F, T4, T5 and T6 temper conditions used in this study.
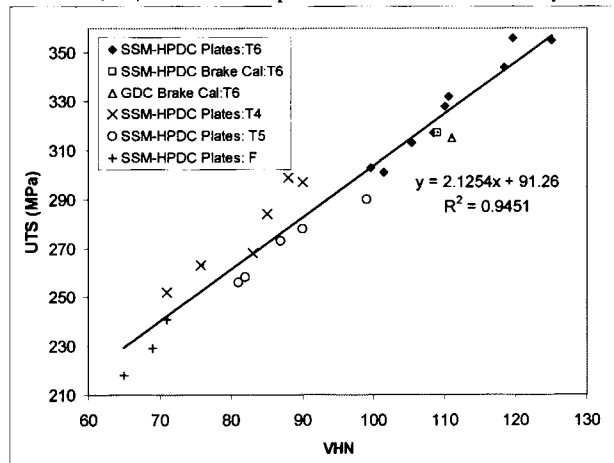

Figure 5. Correlation between UTS and VHN for Al-7Si-Mg alloys in the F, T4, T5 and T6 temper conditions used in this study.

From Figure 4 it is seen that the correlation between YS and hardness is reasonable in the range of hardness and yield strengths tested. From Figure 5 it is seen that the correlation between UTS and hardness is comparable to that of YS and hardness in Fig. 4. The reason why better correlation with UTS is not obtained with Al-7Si-Mg alloys is most likely due to the fact that the UTS is influenced by the degree of spheroidisation of the eutectic Si particles in these alloys. Spheroidised Si-particles tend to result in a higher % elongation, which in turn gives a higher UTS as necking generally does not occur. The data points in Fig. 5 include alloys in which the eutectic Si particles are fibrous (F and T5) and spheroidised (T4 and T6), resulting in a worse-than-expected correlation between UTS and VHN. This suggestion is supported by the fact that most of the F and T5 data points lie below the trend line in Fig. 5, whereas the T4 (and to a lesser extent the T6) data points are above the trend line.

An equation has been proposed before to convert Brinell hardness of alloys A356 to A357 to YS by employing the strain hardening exponent (n) [18]. Accurate n-values from experimental data in

this study could not be obtained due to the removal of the extensometer during tensile testing after reaching the 0.2% plastic strain value. However, assuming that the strain hardening exponent is constant over the plastic strain range up to the point of necking during tensile testing of these alloys, an expression for YS/UTS in terms of n alone may be found (eq. 4):

$$YS_{0.2\%}/UTS \approx \{(0.002)^n (\exp n)\} /(n)^n \qquad (4)$$

Equation 4 is derived from the Hollomon equation ($\sigma = K\varepsilon^n$), as well as from the conversion equations for engineering strain (e) to true strain (ε) [$\varepsilon = \ln (e+1)$], engineering stress (s) to true stress (σ) [$\sigma = s(e+1)$] and the equivalence of true strain at necking = n. Using the data points in Fig. 4 and their respective UTS values in Fig. 5, average n-values for each temper condition can be calculated (Table III).

Table III. Average n-values for Al-7Si-Mg alloys in this study in different temper conditions

Temper condition	Average n-value	Standard deviation
F	0.188	0.0015 from 3 values
T4	0.165	0.0065 from 6 values
T5	0.125	0.0071 from 5 values
T6	0.072	0.0083 from 11 values

The n-values presented in Table III correspond well to those that could be found in the literature, validating the use of eq. 4. Bogdanoff and Dahlström [20] found n-values of 0.17-0.22 for as-cast A356. The evaluated strain hardening exponent for A356/7-T6 according to Wang [21] ranged from 0.045-0.095 depending on the secondary dendrite arm spacing. Rometsch and Schaffer [18] found n-values of 0.088 and 0.078 for their A356 and A357 alloys in the T6 temper condition respectively.

Minimizing $\Sigma(YS_{Measured} - YS_{Predicted})^2$ and ensuring that the intercept of the line of best fit passes through the origin, equation 5 is proposed:

$$YS = 3.03 \times VHN \times [0.055]^n \qquad (5)$$

The predicted YS-values using this equation correlate very well with the measured YS-values (Fig. 6).
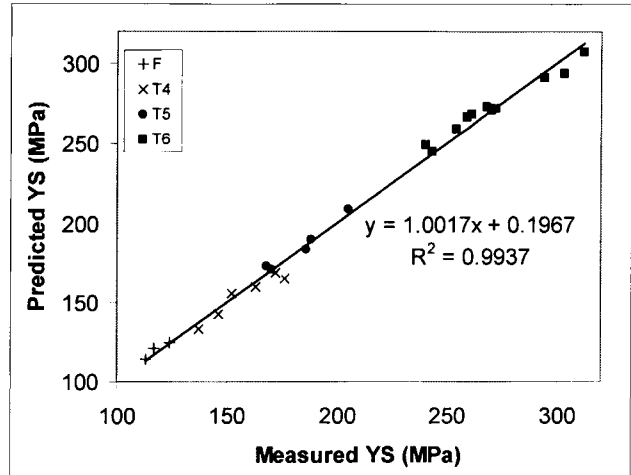

Figure 6. Plot of predicted YS from VHN data (eq. 5) against measured YS for Al-7Si-Mg alloys in the F, T4, T5 and T6 temper conditions used in this study.

ASTM Standard B969-10 specifies that SSM-processed A356 should be artificially aged at 160°C for 3-6 h to obtain the T6 temper condition (Table 2). However, Fig. 7 shows that at 160°C, a time of 29 h would be required to obtain peak properties, which also simultaneously gives similar properties in this alloy regardless of natural pre-aging or no such aging. Using the specified times of 3-6 h according to ASTM B969-10 will result in a large variation in tensile properties in the different naturally pre-aged alloys, in contrast to when an artificial aging time of 29 h is used. Artificial aging at 170°C for 6 h for alloys A357 or F357 will result in a similar situation [12]. According to this study, the specified times to achieve the T6 condition in ASTM B969-10 probably need to be revised. The nanostructural evolution of Al-7Si-Mg alloys after artificial aging with and without natural pre-aging has recently been characterized by the authors using transmission electron microscopy and atom probe tomography and correlated with hardness and mechanical tensile properties [19].
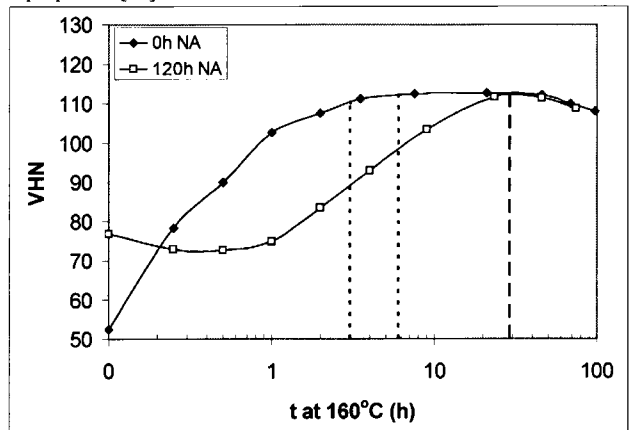

Figure 7. Artificial aging curves of SSM-HPDC alloy A356 (0.34% Mg) at 160°C following no or 120 h natural pre-aging, showing specified aging times of 3-6 h according to ASTM B969-10, as well as 29 h.

470

An artificial aging time of 29 h may be prohibitively long and therefore artificial aging parameters of 180°C for 4 h are suggested as the optimum for SSM-HPDC alloys A356 and F357 [7-12] and for dendritic A356 and F357 [11,13], without a significance decrease in hardness compared to 160°C (Fig. 8).
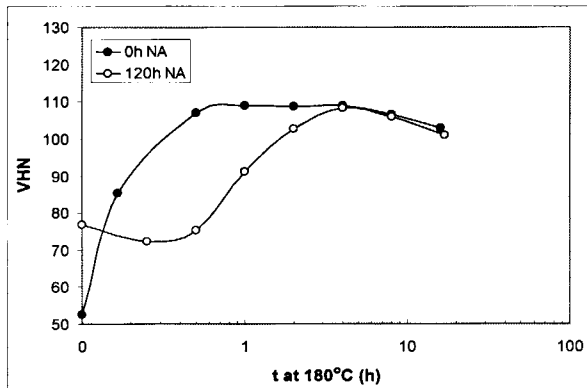

Figure 8. Artificial aging curves of SSM-HPDC alloy A356 (0.34% Mg) at 180°C following no or 120 h natural pre-aging.

Conclusions

- The stability of the Mg-containing π-phase in alloy F357 causes a reduction in the amount of magnesium in solid solution. This has a detrimental effect on the aging behaviour of this alloy compared to alloy A356.

- The strength and macrohardness values of Al-7Si-Mg alloys show good linear relationships to (at% Mg-concentration available for precipitation hardening)$^{1/2}$.

- The aging response of Al-7Si-Mg alloys is not influenced by having a globular or dendritic microstructure.

- The frequently specified artificial aging parameters of 160°C for 3-6 h or 170°C for 6 h for both dendritic and globular Al-7Si-Mg alloys will result in large variations in properties depending on the natural pre-aging period. Parameters of 180°C for 4 h are proposed as an alternative to overcome this shortcoming.

References

1. Ian Polmear, *Light alloys: from traditional alloys to nanocrystals* (Oxford: Butterworth-Heinemann, 2006), 221-224.
2. D. Liu, H.V. Atkinson, P. Kapranos, W. Jirattiticharoean, and H. Jones, "Microstructural evolution and tensile mechanical properties of thixoformed high performance aluminium alloys," *Materials Science and Engineering A*, 361 (2003), 213-224.
3. ASM Specialty Handbook: *Aluminium and Aluminium Alloys* (Materials Park, Ohio: ASM International, 1993), 718-721.
4. C.Y. Yang, S.L Lee, C.K. Lee, and J.C. Lin, "Effects of Be and Fe on the mechanical and corrosion behaviors of A357 alloys," *Materials Chemistry and Physics*, 93 (2005), 412-419.
5. B.A. Dewhirst, "Optimization of the heat treatment of semi solid processed A356 aluminum alloy" (Masters Thesis, Worcester Polytechnic Institute, 2005), 1-5.
6. R. Bruwer, J.D. Wilkins, L.H. Ivanchev, P. Rossouw, and O.F.R.A. Damm (US Patent No. 7368690, 2008).

7. H. Möller, G. Govender, and W.E. Stumpf, "Natural and artificial aging response of semisolid metal processed Al-Si-Mg alloy A356," *International Journal of Cast Metals Research*, 20 (2007), 340-346.
8. H. Möller, G. Govender, and W.E. Stumpf, "Investigation of the T4 and T6 heat treatment cycles of semi-solid processed aluminium alloy A356," *Open Materials Science Journal*, 2 (2008), 11-18.
9. H. Möller, G. Govender, and W.E. Stumpf, "The natural and artificial aging response of semi-solid metal processed alloy A356," *Solid State Phenomena*, 141-143 (2008), 737-742.
10. H. Möller, G. Govender, W.E. Stumpf, and P.C. Pistorius, "Comparison of the heat treatment response of semisolid metal processed alloys A356 and F357," *International Journal of Cast Metals Research*, 23 (2010), 37-43.
11. H. Möller, G. Govender, and W.E. Stumpf, "Application of shortened heat treatment cycles on A356 automotive brake calipers with respective globular and dendritic microstructures," *Transactions of the Nonferrous Metals Society of China*, 20 (2010), 1780-1785.
12. H. Möller, "Optimisation of the heat treatment cycles of CSIR semi-solid metal processed Al-7Si-Mg alloys A356/7" (Doctoral Thesis, University of Pretoria, South Africa, 2011).
13. H. Möller, G. Govender, P. Rossouw, and W.E. Stumpf, "The influence of prior natural aging on the subsequent artificial aging response of aluminium alloy A356 with respective globular and dendritic microstructures," *Advances in Materials Science and Engineering*, 2011, Article ID 375150.
14. J.A. Taylor, D.H. StJohn, and M.J. Couper, "Solution treatment effects in Al-Si-Mg casting alloys," *Aluminum Transactions*, 4-5 (2001), 111-124.
15. C.H. Caceres, J.R. Griffiths, Q.G Wang, and C.J. Davidson, "The effect of Mg on the microstructure and mechanical behavior of Al-Si-Mg casting alloys," *Metallurgical and Materials Transactions A*, 30 (1999), 2611-2618.
16. M. Rosso, E. Romano, P. Giordano, and G.L. Chiarmetta, "Mechanical and microstructural characterization of semi-solid rheocast A356 and A357 aluminum alloys for automotive applications" (Paper presented at the 7th International Conference on Advanced semi-solid processing of alloys and composites, Tsukuba, Japan, 2002), 151-156.
17. M. Badiali, C.J. Davidson, J.R. Griffiths, and A. Zanada, "Fatigue properties of semisolid cast Al-7Si-0.3Mg-T6 alloy" (Paper presented at the 6th International Conference on Semi-solid Processing of Alloys and Composites, Turin, Italy, 2000), 349-354.
18. P.A. Rometsch, and G.B. Schaffer, "An age hardening model for Al-7Si-Mg casting alloys," *Materials Science and Engineering A*, 325 (2002), 424-434.
19. G. Sha, H. Möller, W.E. Stumpf, J.H. Xia, G. Govender, and S.P. Ringer, "Solute-nanostructures and their strengthening effects in Al-7Si-0.6Mg alloy F357" (Submitted to *Acta Materialia*, 2011).
20. T. Bogdanov, and J. Dahlström, "The influence of copper on an Al-Si-Mg alloy A356 - Microstructure and mechanical properties" (Bachelor's thesis, Jönköping University, Sweden, 2009), 33.
21. Q.G. Wang, "Plastic deformation behavior of aluminum casting alloys A356/357," *Metallurgical and Materials Transactions A*, 35 (2004), 2707-2718.